

Synthesis and Structures of Oxyanion Encapsulated Copper(I)–dppm Complexes (dppm = Bis(diphenylphosphino)methane)

Jitendra K. Bera, Munirathnam Nethaji, and Ashoka G. Samuelson*

Department of Inorganic and Physical Chemistry, Indian Institute of Science, Bangalore 560 012, India

Received February 10, 1998

Copper(I)–dppm complexes encapsulating the oxyanions ClO_4^- , NO_3^- , $\text{CH}_3\text{C}_6\text{H}_4\text{CO}_2^-$, SO_4^{2-} , and WO_4^{2-} have been synthesized either by reduction of the corresponding Cu(II) salts and treatment with dppm, or by treating the complex $[\text{Cu}_2(\text{dppm})_2(\text{dmcn})_3](\text{BF}_4)_2$ (**1**) (dmcn = dimethyl cyanamide) with the respective anion. The isolated complexes $[\text{Cu}_2(\text{dppm})_2(\text{dmcn})_2(\text{ClO}_4)]$ (ClO_4) (**2**), $[\text{Cu}_2(\text{dppm})_2(\text{dmcn})_2(\text{NO}_3)]$ (NO_3) (**3**), $\text{Cu}_2(\text{dppm})_2(\text{NO}_3)_2$ (**4**), $[\text{Cu}_2(\text{dppm})_2(\text{CH}_3\text{C}_6\text{H}_4\text{CO}_2)_2]\text{dmcn}\cdot 2\text{THF}$ (**5**), $\text{Cu}_2(\text{dppm})_2(\text{SO}_4)$ (**6**), and $[\text{Cu}_3(\text{dppm})_3(\text{Cl})(\text{WO}_4)]\cdot 0.5\text{H}_2\text{O}$ (**7**) have been characterized by IR, ^1H and $^{31}\text{P}\{^1\text{H}\}$ NMR, UV–vis, and emission spectroscopy. The solid-state molecular structure of complexes **1**, **2**, **4**, and **7** were determined by single-crystal X-ray diffraction. Pertinent crystal data are as follows: for **1**, monoclinic $P2_1/c$, $a = 11.376(10)$ Å, $b = 42.503(7)$ Å, $c = 13.530(6)$ Å, $\beta = 108.08(2)^\circ$, $V = 6219(3)$ Å³, $Z = 4$; for **2**, monoclinic $P2_1/n$, $a = 21.600(3)$ Å, $b = 12.968(3)$ Å, $c = 23.050(3)$ Å, $\beta = 115.97(2)^\circ$, $V = 5804(17)$ Å³, $Z = 4$; for **4**, triclinic $P\bar{1}$, $a = 10.560(4)$ Å, $b = 10.553(3)$ Å, $c = 22.698(3)$ Å, $\alpha = 96.08(2)^\circ$, $\beta = 96.03(2)^\circ$, $\gamma = 108.31(2)^\circ$, $V = 2362(12)$ Å³, $Z = 2$; and for **7**, orthorhombic $P2_12_12_1$, $a = 14.407(4)$ Å, $b = 20.573(7)$ Å, $c = 24.176(6)$ Å, $V = 7166(4)$ Å³, $Z = 4$. Analyses of the crystallographic and spectroscopic data of these complexes reveal the nature of interactions between the Cu^{I} –dppm core and oxyanion. The anchoring of the oxyanion to the $\text{Cu}_n(\text{dppm})_n$ unit is primarily through coordination to the metal, but the noncovalent C–H \cdots O interactions between the methylene and phenyl protons of the dppm and oxygen atoms of the oxyanion play a significant role. The solid-state emission spectra for complexes **1**–**6** are very similar but different from **7**. In CDCl_3 solution, addition of ClO_4^- or NO_3^- (as their tetrabutylammonium salts) to **1** establishes a rapid equilibrium between the anion-complexed and uncomplexed forms. The association constant values for ClO_4^- and NO_3^- have been estimated from the $^{31}\text{P}\{^1\text{H}\}$ NMR spectra.

Introduction

The design and synthesis of smart molecules, able to function as receptors and sensors of charged species, are of immense interest. While cation-receptors have been studied extensively, the design of anion-receptors has been taken up only recently.¹ Due to their varied shapes and sizes,² anions pose a greater challenge than cations. The capture of oxyanions in particular, is difficult due to their large ionic radii, high free energies of solvation and lower Lewis basicities. However, significant advances have been made in the past decade. Beer et al have illustrated the use of metallocene³ and metal–bipyridyl⁴ complexes to synthesize rigid yet modifiable frameworks. The metallocene provides the requisite positive charge and the

appended amide functionalities are hydrogen bond donors. Appropriate functionalization of the metallocene results in selective complexation of anions.^{3a,c} Receptors for even the elusive anion BF_4^- have been designed using iron(II) templates and dinitrile ligands.⁵ Atwood et al have trapped BF_4^- using the bowl shaped cyclooveratrylene (CTV) which is activated for receiving anions by complexation with Ru^{2+} .⁶ The CTV bowl also shows a preferred selectivity for large tetrahedral anions such as MO_4^- ($M = \text{Tc}, \text{Re}$). Surprisingly a preference for TcO_4^- over ReO_4^- has been exhibited by this system.⁷ Thus, most anion-receptors designed till date involve a cationic receptor site with suitable hydrogen bond donors. The CTV system is a notable exception highlighting the power of noncovalent interactions in host–guest chemistry.

Copper(I) complexes are particularly attractive for the design of anion sensors. The flexibility Cu(I) has in the coordination number and geometry requirements⁸—due to the absence of CFSE—should allow the formation of stable complexes with and without the anion. Moreover the lability of these Cu(I)

- (1) (a) Cooper, C. R.; Spencer, N.; James, T. D. *Chem. Commun.* **1998**, 1365. (b) Falana, O. M.; Koch, H. F.; Roundhill, D. M.; Lumetta, G. J.; Hay, B. P. *Chem. Commun.* **1998**, 503. (c) Holman, K. T.; Steed, J. W.; Atwood, J. L. *Angew. Chem., Int. Ed. Engl.* **1997**, *36*, 1736. (d) Jacopozzi, P.; Dalcanele, E. *Angew. Chem., Int. Ed. Engl.* **1997**, *36*, 613. (e) Jagessar, R. C.; Burns, D. H. *Chem. Commun.* **1997**, 1685. (f) Munakata, M.; Wu, L. P.; Yamamoto, M.; Kuroda-Sowa, T.; Maekawa, M. *J. Am. Chem. Soc.* **1996**, *118*, 3117. (g) Gale, P. A.; Sessler, J. L.; Král, V.; Lynch, V. J. *Am. Chem. Soc.* **1996**, *118*, 5140. (h) Atwood, J. L.; Holman, K. T.; Steed, J. W. *Chem. Commun.* **1996**, 1401. (i) Worm, K.; Schmidtchen, F. P. *Angew. Chem., Int. Ed. Engl.* **1995**, *34*, 65. (j) Steed, J. W.; Juneja, R. K.; Atwood, J. L. *Angew. Chem., Int. Ed. Engl.* **1994**, *33*, 2456. (k) Dietrich, B. *Pure Appl. Chem.* **1993**, *65*, 1457.
- (2) Gadre, S. R.; Kölmel, C.; Shrivastava, I. *Inorg. Chem.* **1992**, *31*, 2279.
- (3) (a) Beer, P. D. *Chem. Commun.* **1996**, 689. (b) Beer, P. D.; Drew, M. G. B.; Heseck, D.; Shade, M.; Szemes, F. *Chem. Commun.* **1996**, 2161. (c) Beer, P. D.; Chen, Z.; Goulden, A. J.; Graydon, A.; Stokes, S. E.; Wear, T. J. *Chem. Soc., Chem. Commun.* **1993**, 1834.

- (4) (a) Beer, P. D.; Szemes, F.; Balzani, V.; Salà, C. M.; Drew, M. G. B.; Dent, S. W.; Maestri, M. *J. Am. Chem. Soc.* **1997**, *119*, 11864. (b) Beer, P. D.; Dent, S. W.; Wear, T. J. *J. Chem. Soc., Dalton Trans.* **1996**, 2341. (c) Beer, P. D.; Chen, Z.; Goulden, A. J.; Grieve, A.; Heseck, D.; Szemes, F.; Wear, T. J. *Chem. Soc., Chem. Commun.* **1994**, 1269.
- (5) Mann, S.; Huttner, G.; Zsolnai, L.; Heinze, K. *Angew. Chem., Int. Ed. Engl.* **1996**, *35*, 2808.
- (6) Steed, J. W.; Junk, P. C.; Atwood, J. L.; Barnes, M. J.; Raston, C. L.; Burkhalter, R. S. *J. Am. Chem. Soc.* **1994**, *116*, 10346.
- (7) Holman, K. T.; Halihan, M. M.; Steed, J. W.; Jurisson, S. S.; Atwood, J. L. *J. Am. Chem. Soc.* **1995**, *117*, 7848.

systems make them particularly suited for sensor design. Loss of the ligand and reactivation of the receptor site should be readily possible. We report in this study a set of Cu^{I} -dppm complexes which bind oxyanions through coordination to the metal and weak nonbonding interactions. Our work complements a recent report by Kitagawa et al. on Cu^{I} -diphosphine complexes.⁹ The dimeric structure of $\text{Cu}_2(\text{dppm})_2$ complex with closely spaced copper centers flanked by the phenyl rings of the dppm ligands creates a cavity. The presence of oxyanions—with different charges, sizes, and shapes—in this cavity affects molecular parameters of the $\text{Cu}_2(\text{dppm})_2$ core. A variety of techniques, such as IR stretching frequencies, NMR, and solid-state fluorescence spectra can be used to detect anion complexation.

Experimental Section

Materials. Dichloromethane, petroleum ether (bp 60–80 °C) and acetonitrile were purified and dried by conventional methods, distilled under nitrogen, and deoxygenated before use. Methanol and tetrahydrofuran were distilled and used as such. $[\text{Cu}(\text{CH}_3\text{CN})_4]\text{BF}_4$ and $[\text{Cu}(\text{CH}_3\text{CN})_4]\text{ClO}_4$ were freshly prepared before use. (**Caution!** *Perchlorate salts of metal complexes with organic ligands are potentially explosive. While we have encountered no untoward incident in their preparation and studies, it is preferable that only small amounts are prepared at a time and handled with great caution.*) Bis-(diphenylphosphino)methane, tetrabutylammonium perchlorate, and tetrabutylammonium nitrate were purchased from Aldrich. Dimethyl cyanamide was bought from Fluka. Sodium tungstate and *p*-methyl benzoic acid were obtained from Sisco-Chem (India).

Syntheses. All reactions were carried out in an atmosphere of dried N_2 using standard Schlenk and vacuum line techniques.

Synthesis of $[\text{Cu}_2(\text{dppm})_2(\text{dmcn})_3](\text{BF}_4)_2$ (1). To a CH_2Cl_2 (20 mL) solution containing dppm (0.200 g; 0.52 mmol) was added $\text{Cu}(\text{CH}_3\text{CN})_4\text{BF}_4$ (0.160 g; 0.51 mmol) and stirred at room temperature until it formed a clear solution. It was then treated with dmcn (0.15 mL; 1.85 mmol). After stirring for another 30 min, the solvent was removed under reduced pressure resulting in an oily residue. Trituration with petroleum ether resulted in precipitation of **1** which was filtered and washed with petroleum ether (3 × 5 mL). It was dried under vacuum. Crystallization to get analytically pure material was effected by layering a CH_2Cl_2 solution of the compound with petroleum ether (yield: 94%). Anal. Found (calcd) for $\text{Cu}_2\text{P}_4\text{F}_8\text{N}_6\text{C}_{59}\text{B}_2\text{H}_{62}$: C, 55.36 (55.38); N, 6.57 (6.67); H, 4.89 (4.91). IR data (cm^{-1}): for dppm, 3059 (w), 1579 (w), 1481 (m), 1430 (m), 771 (w), 740 (m), 695 (s), 516 (m), 475 (m); for dmcn, 2235, 2210; for BF_4^- , 1056 (vs, br).

Synthesis of $[\text{Cu}_2(\text{dppm})_2(\text{dmcn})_2(\text{ClO}_4)](\text{ClO}_4)$ (2). Synthesis of **2** was carried out using a procedure identical to the synthesis of **1** starting with $[\text{Cu}(\text{CH}_3\text{CN})_4](\text{ClO}_4)$ instead of $[\text{Cu}(\text{CH}_3\text{CN})_4](\text{BF}_4)$ (yield: 94%). Anal. Found (calcd) for $\text{Cu}_2\text{C}_{56}\text{P}_4\text{N}_4\text{H}_{56}\text{Cl}_2\text{O}_8$: C, 54.46 (54.55); N, 4.54 (4.81); H, 4.58 (4.62). IR data (cm^{-1}): for dppm, 3051 (w), 1583 (w), 1482 (m), 1432 (m), 889 (w), 796 (w), 769 (w), 743 (m), 695 (s), 513 (m), 474 (m); for dmcn, 2237 (s); for ClO_4^- , 1091 (vs, br), 622 (m).

Synthesis of $[\text{Cu}_2(\text{dppm})_2(\text{dmcn})_2(\text{NO}_3)](\text{NO}_3)$ (3). $\text{Cu}(\text{NO}_3)_2$ (0.050 g, 0.27 mmol) was refluxed with copper powder in CH_3CN for 4 h. The colorless solution obtained was filtered to a flask containing dppm (0.200 g, 0.52 mmol) in CH_3CN (5 mL) and stirred for 1 h. The solvent was completely removed under reduced pressure. The white residue was redissolved in CH_2Cl_2 (20 mL), and dmcn (0.15 mL, 1.85 mmol) was added to it. After stirring for 30 min, the solution was concentrated to 2–3 mL. The compound was precipitated by addition of petroleum ether, filtered, and washed with the same solvent (3 × 5 mL). It was then dried under vacuum (yield: 69%). Anal. Found (calcd)

for $\text{Cu}_2\text{P}_4\text{C}_{56}\text{H}_{56}\text{N}_6\text{O}_6$: C, 57.97 (58.13); H, 4.88 (5.09); N, 7.25 (7.46). IR data (cm^{-1}): for dppm, 3051 (w), 1484 (m), 1435 (m), 1096 (m), 763 (m), 694 (m), 517 (m), 477 (m); for dmcn, 2229 (s); for NO_3^- , 1359 (vs, br), 791 (m).

Synthesis of $\text{Cu}_2(\text{dppm})_2(\text{NO}_3)_2$ (4). Tetrabutylammonium nitrate (0.150 g, 0.49 mmol) was added to a solution of **1** (0.190 g, 0.15 mmol) in CH_2Cl_2 (20 mL) and stirred for 2 h. The solvent was removed under reduced pressure, and the residue was washed with petroleum ether. It was redissolved in 5 mL of CH_2Cl_2 , layered with petroleum ether, and kept at 4 °C for 7 days. White crystals of **4** separated out from the solution (yield: 44%). Anal. Found (calcd) for $\text{Cu}_2\text{P}_4\text{C}_{50}\text{H}_{44}\text{N}_2\text{O}_6$: C, 58.88 (58.86); H, 4.36 (4.44); N, 2.75 (2.78). IR data (cm^{-1}): for dppm, 3051 (w), 1484 (m), 1437 (m), 1096 (m), 763 (m), 694 (m), 516 (m), 477 (m); for NO_3^- , 1359 (vs, br), 791 (m).

Synthesis of $[\text{Cu}_2(\text{dppm})_2(\text{CH}_3\text{C}_6\text{H}_4\text{CO}_2)_2]\text{dmcn}\cdot 2\text{THF}$ (5). Potassium *p*-methyl benzoate (0.130 g, 0.75 mmol) was stirred with complex **1** (0.180 g, 0.14 mmol) in 1:1 mixture of $\text{CH}_2\text{Cl}_2/\text{THF}$ (2 × 10 mL) for 12 h. It was then filtered, and the solvent was removed under reduced pressure, resulting in an oily residue. Addition of petroleum ether gave a solid residue which was washed with the same solvent. It was redissolved in dry CH_2Cl_2 (5 mL), filtered, and crystallized by layering with petroleum ether (yield: 51%). Anal. Found (calcd) for $\text{Cu}_2\text{C}_{77}\text{P}_4\text{N}_2\text{H}_{80}\text{O}_6$: C, 66.98 (67.31); H, 5.85 (5.51); N, 2.03 (2.31). IR data (cm^{-1}): for dppm, 3048 (w), 1482 (m), 1435 (m), 771 (m), 736 (s), 695 (s), 513 (m), 479 (m); for dmcn, 2216; for benzoate, 1592 (m) (ring C–C stretch), 1551 (m), 1372 (m) (asymmetric and symmetric CO_2^- stretching, respectively), 906 (w).

Synthesis of $\text{Cu}_2(\text{dppm})_2(\text{SO}_4)$ (6). $\text{CuSO}_4\cdot 5\text{H}_2\text{O}$ (0.120 g, 0.48 mmol) dissolved in CH_3CN with minimum amount of water was refluxed with Cu powder for 10 h. The pale blue colored solution obtained was filtered, and the filtrate was added to dppm (0.370 g, 0.96 mmol) dissolved in CH_3CN (5 mL) and stirred for 2 h. Solvent was removed completely under reduced pressure. The solid residue obtained was redissolved in CH_2Cl_2 (25 mL) and dmcn (0.12 mL, 1.44 mmol) was added to it. After stirring for 30 min, the solution was filtered and concentrated to 2–3 mL. The complex **6** was precipitated by the addition of petroleum ether, filtered, and washed thrice with same solvent (3 × 5 mL). It was then dried under vacuum. Analytically pure material was obtained by recrystallization from a mixture of CH_2Cl_2 and petroleum ether (yield: 45%). Anal. Found (calcd) for $\text{Cu}_2\text{C}_{50}\text{P}_4\text{H}_{44}\text{SO}_4$: C, 60.54 (60.31); H, 4.48 (4.46). IR data (cm^{-1}): for dppm, 3051 (w), 1585 (w), 1481 (m), 1434 (m), 773 (m), 736 (m), 693 (s), 515 (m), 482 (m); for SO_4^{2-} , 1180, 1140, 1095, 612 (m).

Synthesis of $[\text{Cu}_3(\text{dppm})_3(\text{Cl})(\text{WO}_4)]\cdot 0.5\text{H}_2\text{O}$ (7). Complex **1** (0.203 g, 0.16 mmol) and sodium tungstate (0.300 g, 0.91 mmol) were stirred in 1:1 $\text{CH}_2\text{Cl}_2/\text{CH}_3\text{OH}$ (2 × 15 mL) for 2 h. The reaction mixture was filtered, and the colorless filtrate was concentrated under reduced pressure. The residue was redissolved in CH_2Cl_2 and filtered, and the solvent was removed under vacuum to obtain complex **7**. Crystals of **7** were obtained using the procedure employed for preparing crystalline **6** (yield: 34%). Anal. Found (calcd) for $\text{Cu}_3\text{C}_{75}\text{P}_6\text{H}_{66}\text{ClWO}_4\cdot 0.5\text{H}_2\text{O}$: C, 55.08 (55.23); H, 4.08 (4.02). IR data (cm^{-1}): for dppm, 3051 (w), 1585 (w), 1481 (m), 1434 (m), 773 (m), 736 (m), 693 (s), 515 (m), 482 (m);

Complexes $\text{Cu}_2(\text{dppm})_2(\text{CH}_3\text{CN})_4(\text{ClO}_4)_2$ (**8**)¹⁰ and $\text{Cu}_3(\text{dppm})_3(\text{OH})(\text{BF}_4)_2$ ¹¹ were synthesized following literature procedures.

Instruments and Measurements. ¹H NMR spectra were recorded with a Bruker ACF 200 MHz spectrometer operating at 81.1 MHz, and ³¹P{¹H} NMR spectra, on a Bruker AMX 400 MHz spectrometer operating at 162 MHz. Chemical shifts were calibrated to tetramethylsilane and 85% H_3PO_4 as external references for ¹H and ³¹P{¹H} NMR, respectively. All the ¹H and ³¹P{¹H} NMR spectra were recorded in CDCl_3 solution with the exception of **4** and **6**. NMR spectrum of **4** was obtained in acetone-*d*₆ while the ³¹P{¹H} NMR of **6** was recorded in DMSO-*d*₆. ¹H NMR spectrum of complex **6** was recorded from its saturated solution in CDCl_3 . Infrared spectra were measured on a Bio-Rad FTS-7 spectrophotometer. Elemental analyses were done with a Carlo Erba model 1106 elemental analyzer. UV–visible and emission

(8) Hathaway, B. J. *Comprehensive Coordination Chemistry*; Wilkinson, G., Gillard, R. G., McCleverty, J. A., Eds.; Pergamon Press: Oxford, 1987; Vol. 5.

(9) Kitagawa, S.; Kondo, M.; Kawata, S.; Wada, S.; Maekawa, M.; Munakata, M. *Inorg. Chem.* **1995**, *34*, 1455.

(10) Diez, J.; Gamasa, M. P.; Gimeno, J.; Tiripicchio, A.; Camellini, M. *T. J. Chem. Soc., Dalton Trans.* **1987**, 1275.

(11) Ho, D.; Bau, R. *Inorg. Chem.* **1983**, *22*, 4079.

Table 1. Crystallographic Data for [Cu₂(dppm)₂(dmcn)₃](BF₄)₂ (**1**), [Cu₂(dppm)₂(dmcn)₂(ClO₄)]ClO₄ (**2**), Cu₂(dppm)₂(NO₃)₂ (**4**), and [Cu₃(dppm)₃(Cl)(WO₄)]·0.5H₂O (**7**)

	1	2	4	7
empirical formula	C ₅₀ H ₆₂ B ₂ Cu ₂ F ₈ N ₆ P ₄	C ₅₈ H ₅₆ Cl ₂ Cu ₂ N ₄ O ₈ P ₄	C ₅₀ H ₄₄ Cu ₂ N ₂ O ₆ P ₄	C ₇₅ H ₆₆ ClCu ₃ O ₄ P ₆ W
fw	1279.73	1258.93	1019.83	1627.02
crystal system	monoclinic	monoclinic	triclinic	orthorhombic
temp (K)	293	293	293	293
λ (Å)	0.7107	0.7107	0.7107	0.7107
space group	P2 ₁ /c	P2 ₁ /n	P1	P2 ₁ 2 ₁ 2 ₁
a (Å)	11.3760(10)	21.60(3)	10.56(4)	14.407(4)
b (Å)	42.503(7)	12.97(3)	10.55(3)	20.573(7)
c (Å)	13.530(6)	23.05(3)	22.70(3)	24.176(6)
α (deg)			96.08(2)	
β (deg)	108.08(2)	115.97(2)	96.03(2)	
γ (deg)			108.31(2)	
V (Å ³)	6219(3)	5804(17)	2362 (12)	7166(4)
Z	4	4	2	4
ρ _{calcd} (g/cm ³)	1.367	1.441	1.434	1.508
abs coeff (cm ⁻¹)	8.53	9.92	10.87	26.97
F(000)	2632	2592	1048	3264
no. of indep refls	10 916	10 212	8309	6894
no. of data/restraints/parameters	10748/0/678	10212/0/701	8306/0/607	6894/0/286
final R1, ^a wR2 ^b [I > 2σ(I)]	0.0742, 0.1866	0.0778, 0.1731	0.0361, 0.0953	0.1075, 0.2613
final R1, ^a wR2 ^b (all data)	0.1102, 0.2886	0.1549, 0.1927	0.0429, 0.1018	0.2176, 0.2903
GOF ^c	1.073	1.035	1.086	1.015

^a R1 = (Σ||F_o| - |F_c||)/(Σ|F_o|). ^b wR2 = [Σw(|F_o|² - |F_c|²)/Σw|F_o|²]^{1/2}. ^c GOF = [w(F_o² - F_c²)/(n - p)]^{1/2}.

spectra were recorded on Hitachi U-3400 and Hitachi F-2000 spectrophotometers, respectively. Crystals of the complexes were freshly prepared for the emission study.

X-ray Data Collection, Structure Solution, and Refinement.

General. Crystals of **1**, **2**, **4**, and **7** suitable for diffraction studies were glued to the tip of glass fibers and transferred to a computer controlled Enraf-Nonius CAD4 diffractometer with graphite-monochromatized Mo Kα radiation. Accurate unit cell parameters and orientation matrixes were determined by least-squares refinement of 25 well-centered reflections in the range 10° ≤ θ ≤ 18°. Three periodically measured reference reflections showed no significant decay (<5%) during the time of data collection. Crystal data and the relevant experimental details on data collection and refinement for **1**, **2**, **4**, and **7** are given in Table 1. Data collected at 20 °C were corrected for Lorentz and polarization effects. The position of the heavy atoms were determined by Patterson methods using SHELXS86.¹² The remaining atoms were found from difference Fourier analyses using SHELXL-93.¹³

[Cu₂(dppm)₂(dmcn)₃](BF₄)₂ (1**).** A colorless rectangular crystal (0.5 × 0.5 × 0.7 mm) was used for the data collection. A total of 11 784 reflections were collected in the range 1.65° < θ < 24.97°. All non-hydrogen atoms were refined with anisotropic thermal parameters except the carbon atoms of methyl groups on the dmcn ligand and two isolated BF₄⁻ anion fragments. The carbon atom of a methyl group attached to N6 and the fluorine atoms of the anions were found to be severely disordered and they were refined with partial occupancies. Hydrogen atoms were included in the final stage of the refinement on calculated positions bonded on their carrier atoms. An empirical absorption correction was applied to the data.¹⁴ The final difference map shows the highest peak of 0.82 e Å⁻³ located in the vicinity of one of the BF₄⁻ anion. Convergence was reached at R = 0.0742.

[Cu₂(dppm)₂(dmcn)₂(ClO₄)](ClO₄) (2**).** A colorless needle-shaped crystal (0.2 × 0.3 × 0.8 mm) was selected for the X-ray diffraction study. Intensity data of 11096 reflections were collected in the range 1.08° ≤ θ ≤ 24.99°. The structure was found to contain an isolated, disordered ClO₄⁻ along with a complexed anion. All non-hydrogen atoms were refined with anisotropic thermal parameters except the carbon atoms of the methyl groups attached to N4 and atoms of the isolated ClO₄⁻ fragment. The C41 atom was found to be disordered and hence refined with partial occupancies. The electron occupancies

of the oxygen atoms of the isolated ClO₄⁻ unit were found to be disordered over two positions and could be refined with an occupancy factor of 0.5. On the contrary, a very well behaved ClO₄⁻ anion is located inside the metal coordination sphere. All the atoms of the complexed ClO₄⁻ were refined anisotropically with normal thermal parameters. Hydrogen atoms were included in the final stage of the refinement on calculated positions bonded on their carrier atoms. An empirical absorption correction was applied to the data. The highest peak in the final difference map not exceeding 1.0 e Å⁻³ was located near the disordered C41 atom. Convergence was reached at R = 0.0778.

Cu₂(dppm)₂(NO₃)₂ (4**).** A hexagonal block-shaped crystal was cut to measure 0.7 × 0.5 × 0.7 mm and used for the data collection. A total of 8867 reflections were collected in the range 1.65° ≤ θ ≤ 24.97°. All non-hydrogen atoms were refined with anisotropic thermal parameters. Hydrogen atoms were included in the final stage of the refinement on calculated positions bonded on their carrier atoms. The final difference map was flat showing the highest peak of 0.66 e Å⁻³ near Cu1. Convergence was reached at R = 0.0361.

[Cu₃(dppm)₃(Cl)(WO₄)]·0.5H₂O (7**).** A very fragile, stick-shaped crystal was chosen from several crystals mixed with amorphous material. The amorphous material wrapped around the crystal was carefully removed by washing with petroleum ether. Intensity data of 6959 reflections were collected in the range 1.30° ≤ θ ≤ 24.96°. The carbon atoms of the phenyl rings of the dppm ligands were located from the difference Fourier maps and refined as rigid groups. Only the tungsten, coppers and the phosphorus atoms were refined anisotropically. An empirical absorption correction was applied to the data. Hydrogen atoms were included in the final stage of the refinement on calculated positions bonded on their carrier atoms. An isolated partially occupied water molecule was found from the difference Fourier maps. The highest remaining peak in the final difference Fourier was 1.22 e Å⁻³ and located at a distance of 0.659 Å from the Cu₂ center. The final R value obtained was 0.1075.

Results and Discussion

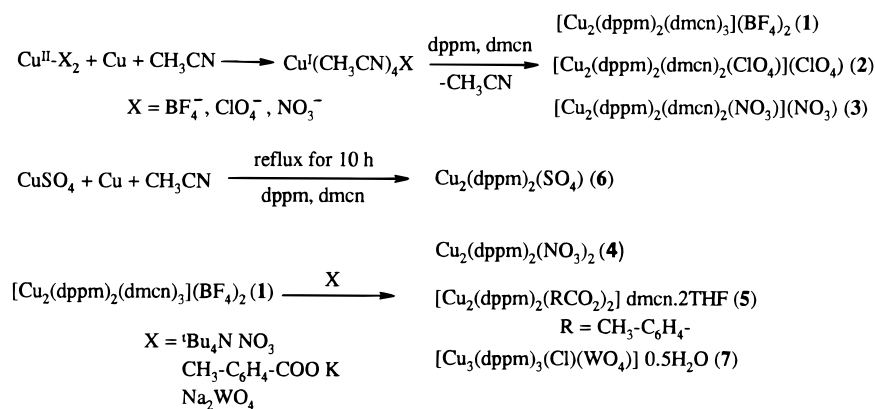
Synthesis and Analysis. Cu^I-dppm complexes encapsulating various oxyanions were prepared starting from the corresponding Cu(II) salt or by treating **1** with the respective anion. The procedures employed in this study have been illustrated in Scheme 1. Complexes **1**, **2**, **3** and **6** were prepared from the corresponding Cu(II) salt. Reduction was carried out by reflux-

(12) Sheldrick, G. M. *SHELXS-86: Program for Crystal Structure Determination*; University of Cambridge: Cambridge, England, 1986.

(13) Sheldrick, G. M. *SHELXL-93: A Program for Crystal Structure Refinement*; University of Göttingen: Göttingen, Germany, 1993.

(14) Parkin, S.; Moezzi, B.; Hope, H. J. *Appl. Crystallogr.* **1995**, *28*, 53.

Scheme 1



ing the Cu(II) salt in acetonitrile with copper powder under nitrogen atmosphere. In the case of **1** and **2**, the intermediate Cu(I) complexes $[\text{Cu}(\text{CH}_3\text{CN})_4]\text{X}$ ($\text{X} = \text{BF}_4^-, \text{ClO}_4^-$) were isolated. Complexes **3** and **6** were prepared by adding dppm and dmcn to the colorless Cu(I) solution obtained in situ after filtering the copper powder. The reduction time varies with the anion present in the reaction mixture. The SO_4^{2-} salt takes the longest and is not completely reduced even after 12 h. Reduction of CuSO_4 is hampered by its poor solubility in CH_3CN . The reduction is facilitated if CuSO_4 is dissolved in a minimum amount of water. Partial reduction in the case of the SO_4^{2-} complex results in a low yield of the complex. Interestingly, although excess dmcn is used in the preparation of complex **6**, the crystalline material does not contain any of the ligand. Complexes **3** and **6**, which do not have the ancillary ligand dmcn have poor solubility in CH_2Cl_2 .

Complexes **4**, **5**, and **7** were prepared starting from **1**. Replacement of the BF_4^- by oxyanions during the reaction was monitored by IR spectroscopy. Complex **1** was reacted with tetrabutylammonium nitrate in CH_2Cl_2 to obtain complex **4**. Copper(I)-dppm complexes containing benzoate or substituted benzoate anion had been synthesized earlier by the reaction of CO_2 with Cu^{I} -aryls in the presence of the diphosphine ligand.¹⁵ Recently, the acetate bridged $\text{Cu}_2(\text{dppm})_2$ complex has been prepared by stirring the $\text{Cu}_3(\text{dppm})_3(\text{OH})(\text{BF}_4)_2$ with sodium acetate.¹⁶ We have prepared complex **5** by replacing the BF_4^- in **1** with *p*-methyl benzoate. The time taken for complete replacement of BF_4^- by the benzoate anion was around 12 h. The decrease in the intensity of BF_4^- bands and the development of new peaks due to the benzoate anion were followed by IR spectroscopy. The composition of **5** included two molecules of THF and one molecule of dmcn. This was confirmed by ^1H NMR and chemical analysis.

Complex **7** was prepared by treating **1** with Na_2WO_4 in 1:1 $\text{CH}_2\text{Cl}_2/\text{CH}_3\text{OH}$ solvents. Complete replacement of BF_4^- was confirmed by the IR spectra and the analytical data. Abstraction of Cl^- from the chlorinated solvent in the presence of sodium salts is known.¹⁷ In this case also, CH_2Cl_2 is the probable source of Cl^- .

The composition of complexes **3** and **4** bring out some interesting features regarding the interaction of dmcn and NO_3^-

Chart 1

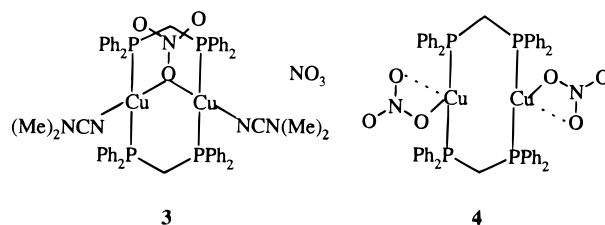
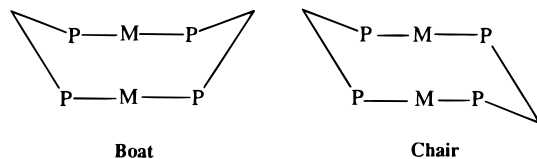


Chart 2



with the $\text{Cu}_2(\text{dppm})_2$ system (Chart 1). Complex **3** was prepared in the presence of excess dmcn and the ratio of Cu(I) and NO_3^- was 1:1. Use of excess dmcn results in formation of **3** containing two dmcn and one NO_3^- inside the metal coordination sphere.¹⁸ On the contrary, treatment of complex **1**, which has 1.5 equivalent of dmcn for each Cu(I), with excess NO_3^- gives **4**. Complex **4** does not contain any dmcn and both NO_3^- ions are bonded to copper. This illustrates the labile nature of both NO_3^- and dmcn, which allows formation of either **3** or **4** depending on the ratio of the reagents used.

Solid-State Molecular Structure. X-ray structure determination was carried out to confirm the nuclearity and understand the nature of the interaction between the anions and Cu^{I} -dppm core. Single crystals suitable for X-ray diffraction study were obtained for **1**, **2**, **4**, and **7** and their molecular structure were established. We discuss the common features observed in these complexes first. The structural details unique for the individual complexes are discussed later.

The solid-state molecular structure of complexes **1**, **2**, and **4** consists of a dimeric $\text{Cu}_2(\text{dppm})_2$ core while complex **7** is a trimeric $\text{Cu}_3(\text{dppm})_3$ unit. In the dimeric complexes, two copper atoms are doubly bridged by two dppm ligands to form an eight-membered $\text{Cu}_2\text{P}_4\text{C}_2$ ring. The $\text{Cu}_2\text{P}_4\text{C}_2$ ring can adopt both boat and chair conformations. If the methylene carbons are cis, they have a boat conformation and if they are trans, a chair conformation results (Chart 2). Several structurally characterized $\text{Cu}_2(\text{dppm})_2$ complexes are in the boat form.^{16,19} Recently Walton *et al.* have solved the structure of $[\text{Re}_2(\text{dppm})_2]$ units

(15) Marsich, N.; Camus, A.; Nardin, G. *J. Organomet. Chem.* **1982**, 239, 429.

(16) Harvey, P. D.; Drouin, M.; Zhang, T. *Inorg. Chem.* **1997**, 36, 4998.

(17) (a) Pérez-Lourido, P. A.; García-Vázquez, J. A.; Romero, J.; Louro, M. S.; Sousa, A.; Chen, Q.; Chang, Y.; Zubieta, J. *J. Chem. Soc., Dalton Trans.* **1996**, 2047. (b) Yam, V. W.-W.; Lee, W.-K.; Lai, T.-F. *Organometallics* **1993**, 12, 2383. (c) Diez, J.; Gamasa, M. P.; Gimeno, J.; Lastra, E.; Aguirre, A.; García-Granda, S. *Organometallics* **1993**, 12, 2213.

(18) The structure of complex **3** is inferred from the spectroscopic and chemical analysis data. The proposed structure is analogous to complex **2** except that the anion is NO_3^- instead of ClO_4^- .

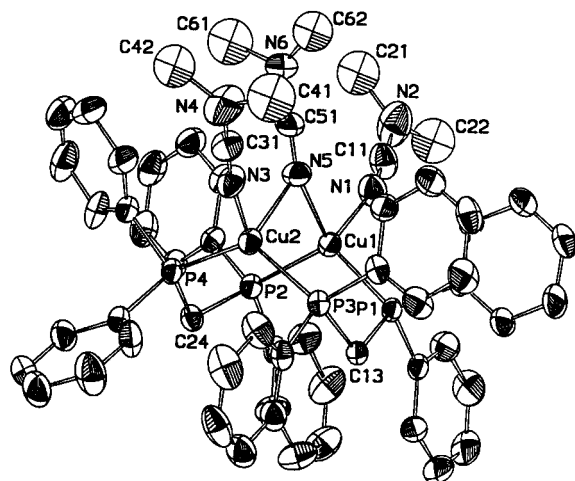


Figure 1. X-ray structure of the $[\text{Cu}_2(\text{dppm})_2(\text{dmcn})_3]^{2+}$ unit in the crystal of **1**. Only one position of the disordered C62 atom is shown. Hydrogen atoms are omitted for clarity.

Table 2. Selected Bond Distances (Å) and Angles (deg) of $[\text{Cu}_2(\text{dppm})_2(\text{dmcn})_3](\text{BF}_4)_2$ (**1**)

Bond Distances			
Cu(1)–Cu(2)	3.143(2)	Cu(2)–P(3)	2.251(2)
Cu(1)–N(1)	2.037(8)	Cu(2)–P(4)	2.255(2)
Cu(1)–N(5)	2.129(6)	Cu(2)–N(5)	2.278(7)
Cu(1)–P(1)	2.245(2)	N(1)–C(11)	1.126(10)
Cu(1)–P(2)	2.270(2)	N(3)–C(31)	1.122(10)
Cu(2)–N(3)	2.034(7)	N(5)–C(51)	1.126(9)
Bond Angles			
N(1)–Cu(1)–N(5)	96.0(3)	N(3)–Cu(2)–P(4)	114.6(2)
N(1)–Cu(1)–P(1)	110.8(2)	P(3)–Cu(2)–P(4)	125.05(7)
N(5)–Cu(1)–P(1)	117.4(2)	N(3)–Cu(2)–N(5)	95.5(3)
N(1)–Cu(1)–P(2)	106.9(2)	P(3)–Cu(2)–N(5)	109.2(2)
N(5)–Cu(1)–P(2)	108.2(2)	P(4)–Cu(2)–N(5)	102.9(2)
P(1)–Cu(1)–P(2)	115.44(7)	Cu(1)–N(5)–Cu(2)	90.9(2)
N(3)–Cu(2)–P(3)	105.4(2)		

in both the chair and boat forms.²⁰ Complexes **1** and **4** adopt a boat conformation with a C13–Cu1–Cu2–C24 torsional angle of -94° and -105° respectively. Complex **2** crystallizes in a chair form with a C13–Cu1–Cu2–C24 torsional angle 132° .

Molecular Structure of 1. The solid-state structure of this complex consists of dinuclear $[\text{Cu}_2(\text{dppm})_2(\eta^1\text{-dmcn})_2(\eta^1, \mu_2\text{-dmcn})]^{2+}$ species and two isolated BF_4^- anions. The molecular structure together with the atomic numbering scheme is depicted in Figure 1. Important bond distances and bond angles are given in Table 2. The coordinating environments of both copper atoms are distorted tetrahedral. Each copper atom is coordinated to two phosphorus atoms of two different dppm ligands and two nitrogen atoms of two dmcn ligands. One dmcn ligand is terminally bonded to each of the copper centers while the other dmcn is bridging the two metal centers. Though the structure of the dimeric moiety of complex **1** looks apparently similar to the reported structure¹⁰ of $\text{Cu}_2(\text{dppm})_2(\text{CH}_3\text{CN})_4(\text{ClO}_4)_2$ (**8**), significant differences are present. In the latter, two acetonitrile ligands are linearly bonded with each copper atom. On the other hand, the solid-state structure of complex **1** has only one terminally bonded dmcn for each copper atom. The bridging dmcn ligand between the two metal centers completes the tetrahedral environment around the metal center (Chart 3).

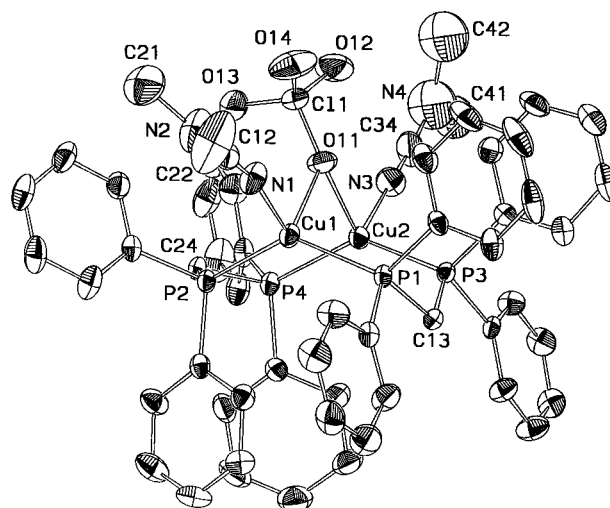


Figure 2. X-ray structure of the $[\text{Cu}_2(\text{dppm})_2(\text{dmcn})_2(\text{ClO}_4)_2]^+$ unit in **2**. Only one position of the disordered C41 atom is shown. Hydrogen atoms are omitted for clarity.

Table 3. Selected Bond Distances (Å) and Angles (deg) of $[\text{Cu}_2(\text{dppm})_2(\text{dmcn})_2(\text{ClO}_4)] \text{ClO}_4$ (**2**)

Bond Distances			
Cu(1)–Cu(2)	3.424(5)	Cu(2)–P(3)	2.246(4)
Cu(1)–N(1)	2.011(6)	Cu(2)–O(11)	2.329(5)
Cu(1)–P(1)	2.247(4)	Cl(1)–O(14)	1.393(6)
Cu(1)–P(2)	2.257(5)	Cl(1)–O(12)	1.402(6)
Cu(1)–O(11)	2.323(5)	Cl(1)–O(13)	1.410(7)
Cu(2)–N(3)	2.014(7)	Cl(1)–O(11)	1.455(5)
Cu(2)–P(4)	2.241(5)		
Bond Angles			
N(1)–Cu(1)–P(1)	108.2(2)	N(3)–Cu(2)–P(3)	106.7(2)
N(1)–Cu(1)–P(2)	107.2(2)	P(4)–Cu(2)–P(3)	133.47(13)
P(1)–Cu(1)–P(2)	131.09(13)	N(3)–Cu(2)–O(11)	100.7(3)
N(1)–Cu(1)–O(11)	100.8(3)	P(4)–Cu(2)–O(11)	104.27(14)
P(1)–Cu(1)–O(11)	102.7(2)	P(3)–Cu(2)–O(11)	98.93(14)
P(2)–Cu(1)–O(11)	102.73(14)	Cu(1)–O(11)–Cu(2)	94.8(2)
N(3)–Cu(2)–P(4)	107.9(2)		

The copper–phosphorus distances are marginally shorter than those observed in the acetonitrile complex **8** (2.283 and 2.270 Å). The Cu1–N1 and Cu2–N3 distances are similar and shorter than the Cu–N5 distances observed for the bridging nitrogen atom. Moreover, Cu1–N5 and Cu2–N5 distances are not equal adding to the asymmetry around the copper centers. The distorted tetrahedral environment around both metal centers is evident from the angles reported in Table 2. The P1–Cu1–P2 and P3–Cu2–P4 angles are larger than the ideal tetrahedral value of 109° . The obvious consequences are the narrowing of the N1–Cu1–N5 and N3–Cu2–N5 angles.

Molecular Structure of 2. The solid-state structure of the above complex can be described as a discrete cationic $[\text{Cu}_2(\text{dppm})_2(\eta^1\text{-dmcn})_2(\eta^1, \mu_2\text{-OClO}_3)]^+$ species and an isolated ClO_4^- anion. The structure together with the atomic numbering scheme is depicted in Figure 2. Important bond distances and bond angles are given in Table 3. The most interesting feature of this structure is the inclusion of the perchlorate anion inside the coordination sphere of the metals. The structure of the dimeric cationic unit is similar to that of complex **1** except for the fact that the bridging dmcn ligand is replaced by the ClO_4^- anion (Chart 3). The oxygen atom of the perchlorate anion forms a bridge between two copper centers in η^1, μ_2 fashion. Similar bond distance values of Cu1–O11 and Cu2–O11 indicate the symmetrical nature of this bridge. The P1–Cu1–P2 angle is larger than the ideal tetrahedral value forcing smaller values for O11–Cu1–P1, O11–Cu1–N1, and O11–Cu1–P2.

(19) (a) Blagg, A.; Shaw, B. L.; Thornton-Pett, M. *J. Chem. Soc., Dalton Trans.* **1987**, 769. (b) The structural characterization of a dimeric chloro-bridged complex has confirmed the boat conformation of the $\text{Cu}_2\text{P}_4\text{C}_2$ ring in $\text{Cu}_2(\text{dppm})_2(\text{dmcn})(\text{Cl})_2$ (ref 30).

(20) Wu, W.; Fanwick, P. E.; Walton, R. A. *Chem. Commun.* **1997**, 755.

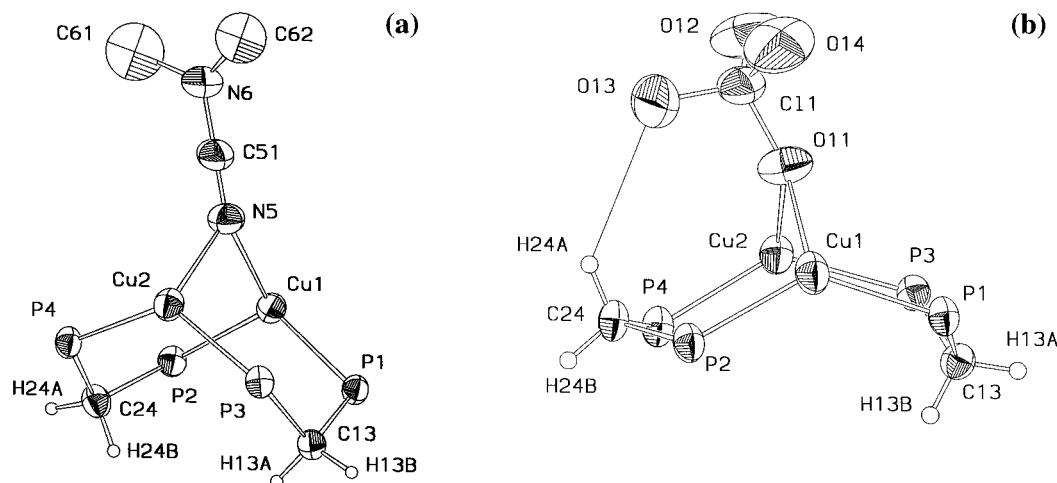
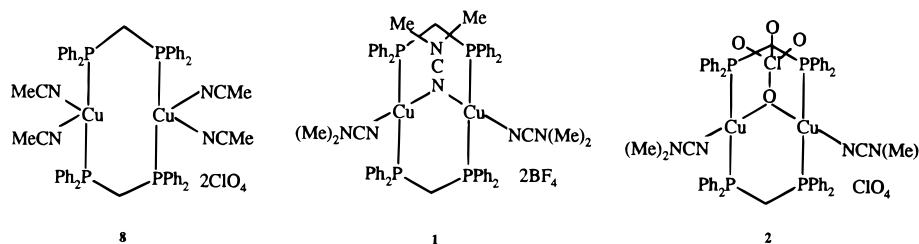


Figure 3. View of the $\text{Cu}_2\text{P}_4\text{C}_2$ ring showing (a) the boat conformation when *dmcn* is the bridging ligand in complex **1** and (b) the chair conformation when ClO_4^- bridges the two Cu centers in complex **2**. The interaction between H24A and O13 in complex **2** is shown by the solid line.

Chart 3



The spherical nature of ClO_4^- often results in a very high degree of thermal motion even in the solid state. Although the constituting oxygen atoms of the ClO_4^- outside the metal coordination sphere in complex **2** are severely disordered, the encapsulated ClO_4^- exhibits *normal* thermal motion. Careful inspection of the structure reveals that the oxygen atoms of the complexed ClO_4^- engage in weak hydrogen bonding $\text{C}\cdots\text{H}\cdots\text{O}$ interactions²¹ with the methylene and the phenyl protons of the *dppm* ligands. The $\text{C}\cdots\text{O}$ distances are in the range of 3.426(9)–3.784(12) Å. These weak interactions help to anchor the ClO_4^- inside the cavity generated by the $\text{Cu}_2(\text{dppm})_2$ core which results in normal thermal parameters for the oxygen atoms of the included oxyanion.

Another unique feature of this structure is the chair conformation of the $\text{Cu}_2\text{P}_4\text{C}_2$ ring. The change in the conformation from boat to chair on changing the bridging ligand *dmcn* (**1**) to ClO_4^- (**2**) is remarkable. The difference in the conformation is due to the presence of ClO_4^- inside the cavity which is tilted toward the methylene bridge (C24). One of the perchlorate oxygens (O13) makes a short contact with H24A. This interaction would not be possible if the complex had the boat structure where both C13 and C24 stay on opposite sides of the bridging ligand (Figure 3a and 3b).

Molecular Structure of 4. The solid-state structure of this complex consists of neutral dinuclear $[\text{Cu}_2(\text{dppm})_2(\eta^1\text{-ONO}_2)_2]$ units. The molecular structure together with the atomic numbering scheme is depicted in Figure 4. Important bond distances and angles are given in Table 4. The coordination environment around the copper centers are quite similar and can be considered as distorted trigonal with two phosphorus atoms of different *dppm* units and an oxygen atom of the nitrate anion bonded to

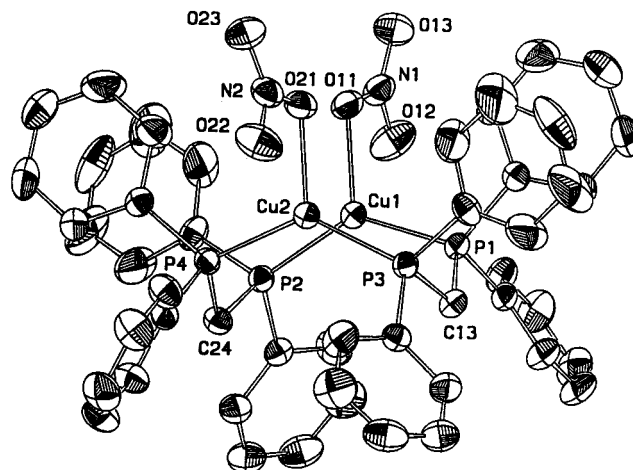


Figure 4. X-ray structure of $\text{Cu}_2(\text{dppm})_2(\text{NO}_3)_2$ (**4**). The hydrogen atoms are omitted for clarity.

it. Surprisingly, copper binds to *dppm* in an asymmetric fashion. The Cu1-P1 and Cu2-P4 are 0.02 Å longer than the Cu1-P2 and Cu2-P3 distances. The Cu1-O11 and Cu2-O21 bond distances are similar and significantly shorter than the Cu1-O12 and Cu2-O22 distances. The short and long Cu-O distances indicate that the NO_3^- unit is bonded to the Cu(I) in a pseudo-bidentate fashion.²²

The P1-Cu1-P2 and P3-Cu2-P4 are greater than 120° . The other angles at Cu1 and Cu2, namely, O11-Cu1-P1 and O21-Cu2-P4 compensate for this widening and are smaller. A closer inspection of the structure reveals some short contacts between the oxygen atoms of the nitrate anion and aryl

(21) (a) Jones, P. G.; Ahrens, B. *Chem. Commun.* **1998**, 2307. (b) Steiner, T. *Chem. Commun.* **1997**, 727.

(22) Wells, A. F. *Structural Inorganic Chemistry*, 4th ed.; The ELBS and Oxford University Press: Oxford, 1975.

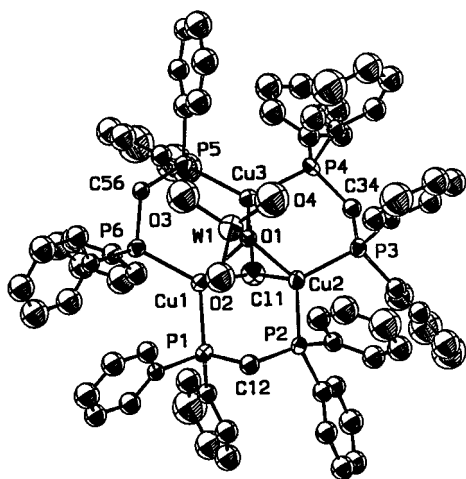


Figure 5. X-ray structure of the Cu₃(dppm)₃(Cl)(WO₄) unit in **7**. The hydrogen atoms are omitted for clarity.

Table 4. Selected Bond Distances (Å) and Angles (deg) of Cu₂(dppm)₂(NO₃)₂ (**4**)

Bond Distances			
Cu(1)–Cu(2)	3.170(4)	Cu(2)–O(22)	2.514(7)
Cu(1)–O(11)	2.108(5)	N(1)–O(13)	1.222(4)
Cu(1)–P(2)	2.239(5)	N(1)–O(12)	1.252(5)
Cu(1)–P(1)	2.256(5)	N(1)–O(11)	1.262(4)
Cu(1)–O(12)	2.511(6)	N(2)–O(23)	1.224(5)
Cu(2)–O(21)	2.108(5)	N(2)–O(22)	1.245(4)
Cu(2)–P(3)	2.239(6)	N(2)–O(21)	1.262(4)
Cu(2)–P(4)	2.257(4)		
Bond Angles			
O(11)–Cu(1)–P(2)	118.3(2)	O(21)–Cu(2)–P(3)	118.3(2)
O(11)–Cu(1)–P(1)	109.9(2)	O(21)–Cu(2)–P(4)	109.8(2)
P(2)–Cu(1)–P(1)	131.78(6)	P(3)–Cu(2)–P(4)	131.79(5)
O(11)–Cu(1)–O(12)	54.2(2)	O(21)–Cu(2)–O(22)	54.0(2)
P(2)–Cu(1)–O(12)	111.8(2)	P(3)–Cu(2)–O(22)	112.0(2)
P(1)–Cu(1)–O(12)	97.25(13)	P(4)–Cu(2)–O(22)	97.2(2)

hydrogens. The short C···O distances are in the range of 3.257(7)–3.476(8) Å.

Molecular Structure of 7. The solid-state structure of the complex **7** consists of a neutral Cu₃(dppm)₃(Cl)₂(η¹-μ₃-OWO₃) unit. The structure together with the atomic numbering scheme is depicted in Figure 5. Important bond distances and bond angles are given in Table 5. The three Cu(I) ions form an isosceles triangle with a dppm ligand bridging each edge to form a Cu₃P₆ core. The chlorine and oxygen atoms are bonded to the three copper atoms in μ₃ mode from opposite faces of the triangle. The Cu–Cl distances are not very different and fall in the range of 2.51–2.56 Å. In contrast, the oxygen atom of the WO₄²⁻ is bonded to the three copper atoms in an asymmetric fashion (Table 5). The copper atoms are tetracoordinate, each being bonded to two phosphorus, one chlorine and one oxygen atom of the WO₄²⁻ unit. The Cu–P distances vary over a small range 2.24–2.27 Å. The Cu₂P₂C rings adopt envelope conformations with the methylene carbon atoms on the flap, one of them folded toward one of the faces and the other two, away from it. This two-up-one-down conformation of dppm ligands is found in analogous trimeric M₃(dppm)₃ clusters.^{11, 23}

The most interesting observation in this structure is the location of WO₄²⁻ inside the cavity formed by the phenyl rings of the dppm ligand. Disposition of the phenyl rings of the dppm ligands in M₃(dppm)₃ complexes is unique. Two phenyl rings attached to a phosphorus center stay on opposite sides of the plane formed by the three metal centers. Therefore, it creates two hydrophobic cavities consisting of six phenyl rings. Several

Table 5. Selected Bond Distances (Å) and Angles (deg) of [Cu₃(dppm)₃(Cl)(WO₄)]·0.5H₂O (**7**)

Bond Distances			
Cu(1)–Cu(2)	3.032(5)	Cu(1)–Cl(1)	2.563(8)
Cu(1)–Cu(3)	3.077(5)	Cu(2)–Cl(1)	2.506(8)
Cu(2)–Cu(3)	3.090(5)	Cu(3)–Cl(1)	2.523(8)
Cu(1)–O(1)	2.25(2)	Cu(1)–P(1)	2.245(7)
Cu(2)–O(1)	2.16(2)	Cu(1)–P(6)	2.269(7)
Cu(3)–O(1)	2.24(2)	Cu(2)–P(3)	2.246(7)
W(1)–O(1)	1.84(2)	Cu(2)–P(2)	2.245(7)
W(1)–O(2)	1.75(2)	Cu(3)–P(4)	2.273(7)
W(1)–O(3)	1.77(3)	Cu(3)–P(5)	2.278(8)
W(1)–O(4)	1.71(3)		
Bond Angles			
O(4)–W(1)–O(2)	110.7(13)	P(3)–Cu(2)–P(2)	118.5(3)
O(4)–W(1)–O(3)	109(2)	O(1)–Cu(2)–Cl(1)	84.1(5)
O(2)–W(1)–O(3)	106.3(12)	P(3)–Cu(2)–Cl(1)	101.8(3)
O(4)–W(1)–O(1)	105.7(11)	P(2)–Cu(2)–Cl(1)	117.7(3)
O(2)–W(1)–O(1)	111.4(9)	O(1)–Cu(3)–P(4)	116.4(4)
O(3)–W(1)–O(1)	113.4(11)	O(1)–Cu(3)–P(5)	107.4(4)
P(1)–Cu(1)–O(1)	114.0(5)	P(4)–Cu(3)–P(5)	124.6(3)
P(1)–Cu(1)–P(6)	122.2(3)	O(1)–Cu(3)–Cl(1)	82.1(4)
O(1)–Cu(1)–P(6)	111.8(5)	P(4)–Cu(3)–Cl(1)	101.9(3)
P(1)–Cu(1)–Cl(1)	105.5(3)	P(5)–Cu(3)–Cl(1)	116.6(3)
P(6)–Cu(1)–Cl(1)	114.9(3)	Cu(2)–Cl(1)–Cu(3)	75.8(2)
O(1)–Cu(2)–P(3)	117.8(5)	Cu(2)–Cl(1)–Cu(1)	73.5(2)
O(1)–Cu(2)–P(2)	111.8(5)	Cu(3)–Cl(1)–Cu(1)	74.5(2)

“noncoordinating” anions such as CF₃SO₃⁻,²⁴ SO₄²⁻,²⁵ and PF₆⁻²⁶ have been trapped inside this cavity and the anion-binding activity of the Cu₃(dppm)₃ core has been highlighted recently.²⁷ The cationic metal centers act as soft Lewis-acid centers and the phenyl groups of dppm anchors the anion through noncovalent interactions. In complex **7**, the O11 atom is bonded to the three copper centers. The spherical WO₄²⁻ is engaged in weak hydrogen bonding interactions with the methylene and the phenyl protons of the dppm ligand, similar to the oxyanions ClO₄⁻ and NO₃⁻. The C···O distances are in the range of 3.118–3.737 Å.

- (23) (a) Xiao, J.; Hao, L.; Puddephatt, R. J.; Manojlovic-Muir, L.; Muir, K. W. *J. Am. Chem. Soc.* **1995**, *117*, 6316. (b) Hao, L.; Xiao, J.; Vittal, J. J.; Puddephatt, R. J. *Angew. Chem., Int. Ed. Engl.* **1995**, *34*, 346. (c) Maekawa, M.; Munakata, M.; Kuroda-Sowa, T.; Hachiya, K. *Inorg. Chim. Acta* **1995**, *233*, 1. (d) Xiao, J.; Kristof, E.; Vittal, J. J.; Puddephatt, R. J. *J. Organomet. Chem.* **1995**, *490*, 1. (e) Xiao, J.; Puddephatt, R. J.; Manojlovic-Muir, L.; Muir, K. W. *J. Am. Chem. Soc.* **1994**, *116*, 1129. (f) Rashidi, M.; Kristof, E.; Vittal, J. J.; Puddephatt, R. J. *Inorg. Chem.* **1994**, *33*, 1497. (g) Mirza, H. A.; Vittal, J. J.; Puddephatt, R. J. *Inorg. Chem.* **1993**, *32*, 1327. (h) Lloyd, B. R.; Manojlovic-Muir, L.; Muir, K. W.; Puddephatt, R. J. *Organometallics* **1993**, *12*, 1231. (i) Xiao, J.; Vittal, J. J.; Puddephatt, R. J.; Manojlovic-Muir, L.; Muir, K. W. *J. Am. Chem. Soc.* **1993**, *115*, 7882. (j) Manojlovic-Muir, L.; Muir, K. W.; Mirza, H. A.; Puddephatt, R. J. *Organometallics* **1992**, *11*, 3440. (k) Jennings, M. C.; Puddephatt, R. J.; Manojlovic-Muir, L.; Muir, K. W.; Mwariri, B. N. *Organometallics* **1992**, *11*, 4164. (l) Puddephatt, R. J.; Manojlovic-Muir, L.; Muir, K. W. *Polyhedron* **1990**, *9*, 2767. (m) Franzoni, D.; Pelizzi, G.; Predieri, G.; Tarasconi, P.; Vitali, F.; Pelizzi, C. *J. Chem. Soc., Dalton Trans.* **1989**, 247. (n) Manojlovic-Muir, L.; Muir, K. W.; Lloyd, B. R.; Puddephatt, R. J. *J. Chem. Soc., Chem. Commun.* **1983**, 1336. (o) Bresciani, N.; Marsich, N.; Nardin, G.; Randaccio, L. *Inorg. Chim. Acta* **1974**, *10*, L5. The two-up-one-down conformation of the Cu₂P₂C₂ ring also noted in the solid-state structure of the complexes Cu₃(dppm)₃(μ³-Br)₂ClO₄ and Cu₃(dppm)₃(μ³-I)₂I (ref 30). (24) Knoepfler, A.; Wurst, K.; Peringer, P. *J. Chem. Soc., Chem. Commun.* **1995**, 131. (25) Hämmerle, B.; Müller, E. P.; Wilkinson, D. L.; Müller, G.; Peringer, P. *J. Chem. Soc., Chem. Commun.* **1989**, 1527. (26) In a recent publication, Harvey et al. have shown that even an elusive anion PF₆⁻ can be trapped inside the cavity generated by the Pd₃(dpam) core where dpam (Ph₂As–CH₂–AsPh₂) is an arsenic analogue of dppm (Zhang, P.; Drouin, M.; Harvey, P. D. *Chem. Commun.* **1996**, 877). In the solid-state structure of Cu₃(dppm)₃(μ₃-OH)(BF₄)₂ (ref 11), two BF₄⁻ anions are situated in the hydrophobic cavities above and below the Cu₃ triangle. (27) Provencher, R.; Harvey, P. D. *Inorg. Chem.* **1996**, *35*, 2235.

Chart 4

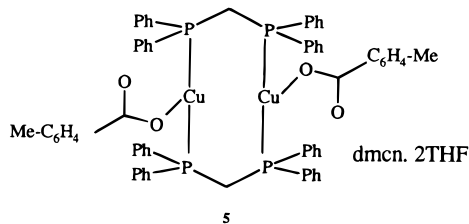
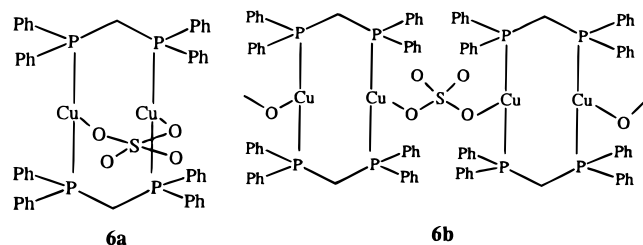


Chart 5



The molecular structure of complex **5** has been proposed on the basis of ^1H and $^{31}\text{P}\{^1\text{H}\}$ NMR, IR, emission spectra, and analysis data. A similar complex containing the unsubstituted benzoate ligand has been characterized structurally.²⁸ The available spectral data of this complex matches with the complex we have synthesized and hence we assume that it adopts a similar structure (Chart 4).

Our efforts to obtain a single-crystal of complex **6**, suitable for X-ray diffraction study were not successful. As a significant amount of water was used during the synthesis, the likelihood of forming a trinuclear species $[\text{Cu}_3(\text{dppm})_3(\mu_3\text{-OH})]\text{SO}_4$ was envisaged. However, this possibility was rejected on the basis of the ^{31}P NMR chemical shift (see discussion of NMR spectra). The IR spectrum of complex **6** indicates the bidentate bridging mode of the SO_4^{2-} to copper. Both structures **6a** and **6b**, fit the spectral and the analysis data (Chart 5). The polymeric structure (**6b**) is more probable considering the fact that it has very poor solubility in chlorinated solvents unlike other dimeric complexes reported in this study.

Variation of Cu–O distances. The Cu–O distances in the oxyanion-coordinated Cu^{I} –dppm complexes show a large variation depending on the nature of oxyanion and the mode of binding. The ClO_4^- ion coordinates in different modes depending on the separation between the two copper centers. The Cu–Cu, Cu–O distances and the corresponding coordination modes of ClO_4^- have been shown in Figure 6a–c. The Cu–O distances are in the range 2.236(6)–2.435(8) Å.⁹ Interestingly, much smaller Cu–O values are obtained with NO_3^- bonded to copper. In complex **4**, the NO_3^- is η^1 bonded (Figure 6d). Recently a similar Cu^{I} –dppm complex with η^2, μ_2 -bonded NO_3^- has been structurally characterized (Figure 6e).²⁹ The Cu–O bond distance in this complex (2.183(5) Å) is longer than that in complex **4** (2.108(5) Å). Short Cu–O distances are observed in the Cu^{I} –benzoate (2.002(4) Å)²⁸ and Cu^{I} –acetate (1.993(4) Å)¹⁶ complexes (Figure 6f). The variation of the Cu–O distances can be rationalized on the basis of the charge density on the coordinating atom. The greater the charge on the coordinating atom, the shorter the Cu–O distance and better is the interaction. The strengths of the Cu–O interaction based on the Cu^I–O distances are as follows: acetate, benzoate > nitrate >

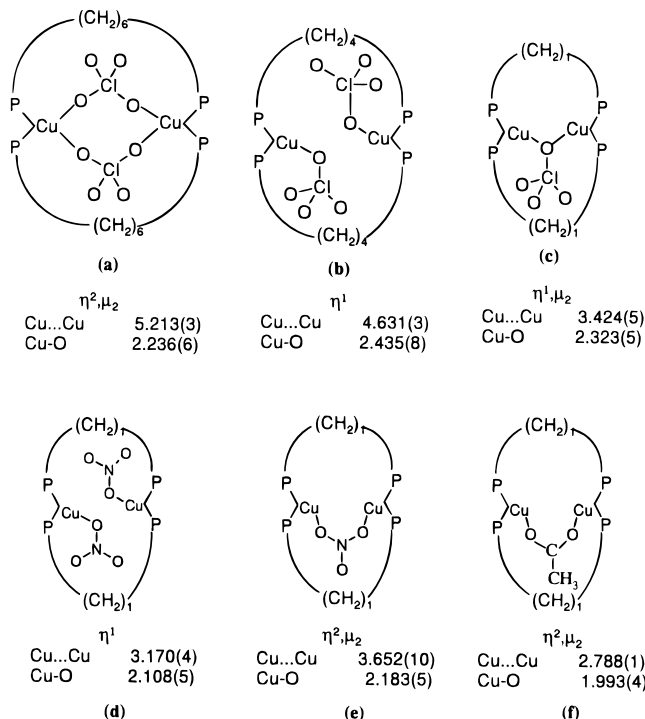


Figure 6. Schematic representation of the structurally characterized dimeric Cu^{I} –diphosphine complexes coordinating ClO_4^- (a–c), NO_3^- (d, e), and acetate anion (f). The corresponding Cu...Cu and Cu–O distances are also given. Values are taken from ref 10 (a and b), this work (c and d), ref 29 (e), and ref 16 (f).

perchlorate. Similarly among the trimeric complexes, the Cu–O distances in complex **7** are in the range 2.16(2)–2.25(2) Å and much longer than that observed in $\text{Cu}_3(\text{dppm})_3(\text{OH})(\text{BF}_4)_2$ (1.996–2.026 Å).¹¹

The Cu1–Cu2 distances in complexes **1**, **2**, and **4** are much shorter compared to that observed in complex **8** (3.757 Å).¹⁰ The large reduction in the metal–metal separation (0.61 Å) in complex **1** due to the presence of a bridging dmca ligand between the two copper centers is significant. The separation increases by 0.28 Å when the bridging dmca ligand is replaced by the ClO_4^- unit. Similarly, the bridging mode of nitrate causes a significant difference in the Cu–Cu distances (3.170(4) and 3.652(10) Å for complex **4** and the η^2, μ_2 -bonded NO_3^- complex, respectively). This is a consequence of the different modes of bonding adopted by NO_3^- in the two complexes. The ligand-controlled Cu–Cu distance in dimeric and trimeric Cu^{I} –dppm complexes have been discussed in detail by us recently.³⁰

Solid-State IR Spectra. All the complexes in the solid-state exhibit usual infrared absorptions characteristic of the ligands present and the associated anionic moiety. Two closely spaced bands separated by 25 cm^{-1} corresponding to $\text{C}\equiv\text{N}$ stretching frequencies of the terminal and bridging dmca ligands are observed in the IR spectra of complex **1**. Such splitting is not observed in the IR spectrum of complex **2** where both dmca ligands are terminal. Surprisingly, the ClO_4^- encapsulated in the cavity of this complex could not be distinguished from that outside using IR spectroscopy. However, a comparison of the IR spectra of complex **2** with other $\text{Cu}_2(\text{dppm})_2$ complexes³¹

(30) Bera, J. K.; Nethaji, M.; Samuelson, A. G. *Inorg. Chem.* **1999**, *38*, 218.

(31) The IR spectrum of complex **2** was compared with those of complexes **1**, **4**, and $\text{Cu}_2(\text{dppm})_2(\text{dmca})(\text{Cl})_2$. It is to be noted that the $\text{Cu}_2\text{P}_2\text{C}_4$ ring in all these complexes adopt a boat conformation with the sole exception of complex **2** which has a chair conformation in the solid state.

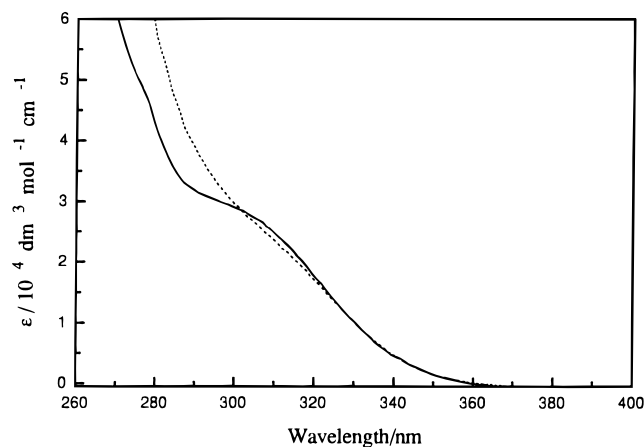
(28) Lanfredi, A. M. M.; Ugozzoli, F.; Camus, A.; Marsich, N.; Capelletti, R. *Inorg. Chim. Acta* **1993**, *206*, 173.

(29) Ruina, Y.; Kunhua, L.; Yimin, H.; Dongmei, W.; Douman, J. *Polyhedron* **1997**, *16*, 4033.

Table 6. NMR^a and Emission^b Spectral Data of Complexes 1–7

compound	$\delta(^{31}\text{P})$ ($^{31}\text{P}\{^1\text{H}\}$) ^a	$\delta(^1\text{H})$			emission spectra	
		CH ₃ (dmcn)	CH ₂ (dppm)	Ph (dppm)	λ_{max} (emission)	λ_{max} (excitation)
[Cu ₂ (dppm) ₂ (dmcn) ₃](BF ₄) ₂ (1)	-9.98	2.92	3.55	7.12–7.27	470	366
[Cu ₂ (dppm) ₂ (dmcn) ₂ (ClO ₄)](ClO ₄) (2)	-10.89	2.87	3.40	6.92–7.35	470	318
[Cu ₂ (dppm) ₂ (dmcn) ₂ (NO ₃)]NO ₃ (3)	-11.25	2.85	3.28	7.06–7.33	469	362
Cu ₂ (dppm) ₂ (NO ₃) ₂ (4) ^c	-11.00	—	3.39	6.95–7.38	466	380
[Cu ₂ (dppm) ₂ (CH ₃ C ₆ H ₄ CO ₂) ₂] (dmcn)·2THF (5) ^d	-11.76	2.82	3.20	6.75–7.50	468	360 ^e
Cu ₂ (dppm) ₂ (SO ₄) (6)	-9.13 ^f	—	3.39	6.91–7.50	470	380
[Cu ₃ (dppm) ₃ (Cl)(WO ₄)·0.5H ₂ O (7)	-14.61	—	3.26	6.92–7.29	510	383

^a Spectra recorded in CDCl₃ unless otherwise stated. ^b Emission spectra were recorded in solid state. ^c Recorded in acetone-*d*₆. ^d Additional peaks are observed at 2.57 (CH₃-benzoate), 7.99, 8.27 (C₆H₄-benzoate), and 1.85, 3.75 (THF). ^e See text. ^f Recorded in DMSO-*d*₆.

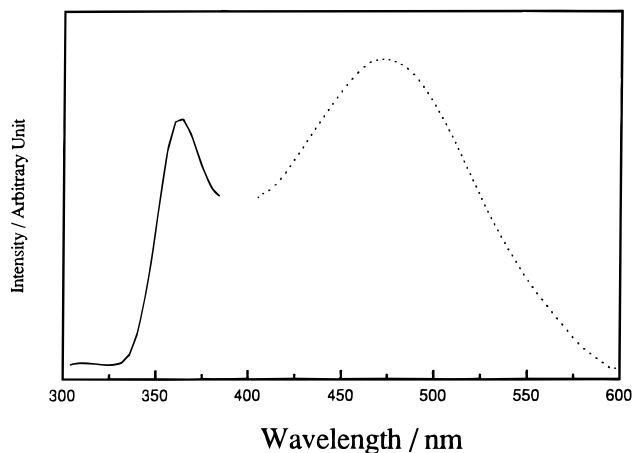
**Figure 7.** UV-vis absorption spectra of **1** (solid line) and **2** (dashed line) in CH₂Cl₂ at room temperature.

shows the presence of two new bands at 889 and 796 cm⁻¹. As these bands are present only in complex **2** and appear in the region of the CH₂ rocking vibration,³² it is likely that they are caused by the unique chair conformation present in this complex.

The IR spectra of complexes **3** and **4** are identical with the exception that **3** also exhibits a sharp absorption at 2229 cm⁻¹ due to the dmcn ligand. Based on the difference in the symmetric and the asymmetric stretching frequencies of the benzoate ligand (186 cm⁻¹),¹⁵ a monodentate binding is inferred²⁸ for complex **5**.

The structure of complex **6** containing the sulfate anion bridging the two copper centers in a bidentate fashion is inferred from the IR spectra. Two closely spaced peaks were observed at 1180 and 1140 cm⁻¹ along with a strong band at 1095 cm⁻¹. A similar observation has been noted for the bidentate SO₄²⁻-bridged cobalt complex.³³

UV-Vis and Emission Spectra. The electronic absorption spectra of all the complexes except **4** and **6** were measured at room temperature in CH₂Cl₂. They are similar and as representative examples, the spectra of complexes **1** and **2** have been given in Figure 7. An intense absorption around 250 nm and a relatively weak absorption around 300 nm dominate the electronic spectra. The luminescence spectra of all the complexes were measured at room temperature in the solid-state. The relevant spectral data are given in Table 6. The luminescence spectrum of complex **1** along with the corresponding excitation spectrum are shown in Figure 8 as representative examples. Complexes 1–6 display emission maxima around 470 nm. Interestingly, though the emission spectra of complexes **1** and

**Figure 8.** Emission (dashed line) and the corresponding excitation (solid line) spectra of a solid sample of **1** at room temperature.

2 are extremely similar, the excitation maxima differ (Table 6). The excitation maximum of complex **2** was observed at 318 nm while no significant emission was noted on irradiation at 362 nm (cf. complexes **1** and **3**). Complex **4** exhibits a broad excitation spectrum with an excitation maximum around 380 nm. The emission band of complex **5** is relatively weak and the excitation spectrum exhibits a very broad absorption ranging from 340 to 380 nm. However, maximum emission occurs on irradiating the sample at 360 nm. The emission spectra of complex **7** is characteristic of trimeric Cu₃(dppm)₃ complexes³⁴ and is completely different from those of the dimeric species reported in this study.

Several assignments such as those involving a phosphine intra-ligand excited state,³⁵ a ligand-to-metal charge transfer state,³⁶ a metal-cluster-centered excited state³⁷ or combinations of these have been made to explain the emission spectra of copper(I) phosphine complexes. The Cu...Cu distances observed in the solid-state structure of **1**, **2**, and **4** are different. If cluster-

(34) The luminescence spectra of trimeric Cu₃(dppm)₃ complexes show a common broad band centered around 510–520 nm. Examples are [Cu₃(dppm)₃(μ₃-OH)](BF₄)₂ (ref 27), [Cu₃(dppm)₃(μ₃-Cl)₂](ClO₄), [Cu₃(dppm)₃(μ₃-Br)₂](ClO₄), and [Cu₃(dppm)₃(μ₃-I)₂](I) (ref 30).

(35) (a) Yam, V. W.-W.; Lee, W.-K.; Cheung, K.-K.; Crystall, B.; Phillips, D. *J. Chem. Soc., Dalton Trans.* **1996**, 3283. (b) Li, D.; Che, C.-M.; Wong, W.-T.; Shieh, S.-J.; Peng, S.-M. *J. Chem. Soc., Dalton Trans.* **1993**, 653.

(36) (a) Yam, V. W.-W.; Lo, K. K.-W.; Cheung, K.-K. *Inorg. Chem.* **1996**, 35, 3459. (b) Yam, V. W.-W.; Fung, W. K.-M.; Cheung, K.-K. *Angew. Chem., Int. Ed. Engl.* **1996**, 35, 1100. (c) Yam, V. W.-W.; Lee, W.-K.; Lai, T.-F. *J. Chem. Soc., Chem. Commun.* **1993**, 1571.

(37) (a) Simon, J. A.; Palke, W. E.; Ford, P. C. *Inorg. Chem.* **1996**, 35, 5, 6413. (b) Li, D.; Yip, H.-K.; Che, C.-M.; Zhou, Z.-Y.; Mak, Thomas C. W.; Liu, S.-T.; *J. Chem. Soc., Dalton Trans.* **1992**, 2445. (c) Barrie, J. D.; Dunn, B.; Hollingsworth, G.; Zink, J. I. *J. Phys. Chem.* **1989**, 93, 3958. (d) Zink, J. I.; Henary, M. *J. Am. Chem. Soc.* **1989**, 111, 7407.

(32) Bacci, M. *Spectrochim. Acta* **1972**, 28A, 2286.

(33) Nakamoto, K. *Infrared spectra of inorganic and coordination compounds*, 3rd ed.; Wiley: New York, 1978.

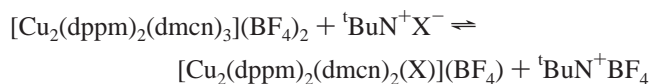
centered transitions are involved, they are likely to be effected by Cu \cdots Cu interactions. The invariance of the emission wavelength rules out the possibility of emission from such a metal-cluster-centered excited state. We tentatively assign the origin of these emission bands to an intra-ligand phosphine excited state. Trimeric complexes also have this relatively weak emission bands around 470 nm along with a strong emission at 510 nm. In fact it is possible to differentiate the dimeric and trimeric Cu^I-dppm complexes on the basis of their emission spectra.³⁰ The photophysical properties of these complexes can be advantageously used in the design of an oxyanion-sensor.

Solution-Phase Study. The ¹H and ³¹P{¹H} NMR spectral data have been summarized in Table 6. Although the solid-state structure of complex **1** shows the presence of both bridging and terminally bonded dmcn in 1:2 ratio, the ¹H NMR spectrum shows a single and sharp methyl signal in solution for all methyl groups. This signal is gradually shifted to higher field when stoichiometric amounts of dmcn is added, suggesting a rapid exchange between the coordinated and noncoordinated dmcn ligands at room temperature. Small but significant changes are observed in the ¹H NMR when complex **1** encapsulates the oxyanions. The methylene protons of dppm show an upfield shift when the bridging dmcn ligand in complex **1** is replaced with ClO₄⁻ to give **2** and NO₃⁻ to give **3** (Table 6). The NMR spectrum of **4** was recorded in acetone-*d*₆ as it was insoluble in CDCl₃ and the methylene protons resonate at δ 3.39 ppm. Complex **5** exhibits the lowest δ value for the methylene proton of the dppm ligand while complex **6** gives a significantly higher value. The trimeric complex **7** shows a δ value of 3.26, typical of other trimeric structures.^{11,23} Phenyl protons of the dppm ligand for all the complexes containing the oxyanions inside the metal coordination sphere resonate over a larger frequency range compared to complex **1**. The weak C-H \cdots O interactions presumably persist in solution resulting in the chemical shift spread.

Though all molecules reported in this paper contain more than one type of (crystallographically different) phosphorus centers, the ³¹P{¹H} NMR spectra of these complexes show only a single resonance. The magnetic equivalence of the phosphorus atoms in solution is consistent with the lability of ligands around Cu(I) and their chemical equivalence. For complex **1**, even at -70 °C, the signal does not split but gradually shifts to a higher field. The upfield shifts noted in the ¹H NMR spectra on replacing the bridging dmcn ligand in **1** by ClO₄⁻ (**2**) and NO₃⁻ (**3**) are observed in the ³¹P{¹H} NMR spectra also (Table 6).

During our study, we have observed a consistently higher negative value in the ³¹P NMR spectra for Cu₃(dppm)₃ complexes compared to Cu₂(dppm)₂ complexes.³⁸ A good comparison is provided by the dimeric **4** and the trimeric [Cu₃(dppm)₃(OH)](BF₄)₂. Although each copper is bonded to two phosphorus atoms and one oxygen atom in both complexes, the ³¹P{¹H} NMR chemical shift for the trimer is -15.26 whereas complex **4** resonates at -11.00 ppm. Consistently, the highest negative value in these series was recorded for the trimeric **7**. This suggests that the ³¹P NMR values can be reliably used to distinguish between dimeric and trimeric structures. The dimeric structure of complex **6** has been assigned from the ³¹P NMR

Scheme 2



data. As a significant amount of water was used to prepare complex **6**, the possibility of forming a trimeric species of the formulas [Cu₃(dppm)₃(OH)](SO₄) was considered. The lowest negative value (-9.13 δ) noted for complex **6** confirms its dimeric structure.

The methylene protons in ¹H NMR (methylene) and the ³¹P-{¹H} signal (P) of the dppm ligand suffer a considerable shift on coordination with Cu(I). The values for the free ligand are 2.82 and -22.68, respectively. The NMR shifts reflect the extent of binding of the dppm ligand with the metal centers. The interaction of an oxyanion with the metal core indirectly influences Cu-P bonding. A stronger interaction (shorter Cu-O distance) with the oxyanion leads to weaker bonding between dppm and the copper (longer Cu-P distance). The chemical shift values of the dppm ligand in solution can then be an indirect measure of the interaction of the anion with copper. The data shown in Table 6 indicates that oxyanions benzoate, ClO₄⁻ and NO₃⁻ coordinate better with the metal core compared to the dmcn ligand. The corresponding values also indicate that the extent of interaction is maximum for benzoate and least for ClO₄⁻. The NO₃⁻ complex has an intermediate value.³⁹

Addition of tetrabutylammonium salt of ClO₄⁻ in excess to **1** causes an upfield shift of the methylene proton. Unfortunately this signal is completely masked by the tetrabutyl protons ranging from 3.25 to 3.29 when NO₃⁻ salt is added to **1**. However, the ³¹P{¹H} NMR signal can be conveniently used to monitor the presence of the anion in the cavity. Addition of the tetrabutylammonium salt of PF₆⁻ to **1** does not change the ³¹P NMR values significantly. However, a gradual shift of the signal is observed while adding stoichiometric amount of tetrabutylammonium salt of either ClO₄⁻ or NO₃⁻ to **1** in CDCl₃ indicating a rapid equilibrium between the anion-complexed and uncomplexed forms (Scheme 2). Association constants were calculated from the resulting titration curves using the program EQNMR.⁴⁰ The values obtained are 249 mol⁻¹ dm³ for ClO₄⁻ and 154 mol⁻¹ dm³ for NO₃⁻. It is interesting to note that though NO₃⁻ coordinates better with Cu(I) (causes a larger shift in ³¹P NMR), ClO₄⁻ forms a thermodynamically more stable complex compared to the planar NO₃⁻. The greater number of oxygen atoms allows many more C-H \cdots O interactions and the tetrahedral disposition of the oxygen atoms make a better fit of the anion in the cavity.

Encapsulation of Oxyanion. It is evident from the structural information and spectroscopic data that Cu_{*n*}(dppm)_{*n*} complexes have the potential to be efficient receptors for oxyanions. The Cu₂(dppm)₂ core forms a cavity generated by the phenyl rings of the dppm ligands with two Lewis-acceptor copper centers inside it. The entry of oxyanion to the cavity is initiated by the coordinate-bond formation with the copper ions. Inside the cavity, the oxyanion is locked by multiple hydrogen bonding interactions. The low crystallographic thermal parameters of the oxygen atoms of the encapsulated oxyanion bear testimony of this fact. For example, a well-behaved ClO₄⁻ was located inside the cavity formed by Cu₂(dppm)₂ cores in complex **2**, although

(38) Consistently larger negative values in the ³¹P NMR spectra are noted for trinuclear Cu₃(dppm)₃ complexes compared to dinuclear Cu₂(dppm)₂ complexes. The values vary over a smaller range of -9.0 to -12.0 ppm in the case of dimers and -14.5 to -22.5 ppm in the case of trimers. One exception among dimers is complex Cu₂(dppm)₂(dmcn)(Cl)₂ which could exist as a trimer in solution and hence has a chemical shift of -15.2 ppm. For details, see ref 30.

(39) As the NMR spectrum of complex **4** could only be recorded in acetone-*d*₆, the value could not be compared with others. The methylene peaks of the Cu^I-dppm complexes undergo considerable downfield shift when acetone-*d*₆ is used as the solvent compared to CDCl₃.

(40) Hynes, M. J. *J. Chem. Soc., Dalton Trans.* **1993**, 311.

the oxygen atoms of ClO₄⁻ outside the metal coordination sphere were severely disordered. Significant structural changes of the host Cu₂(dppm)₂ core are also observed as a result of encapsulation. The methylene and the phenyl hydrogens protons of the dppm ligands orient themselves toward the cavity in complex **2** in which ClO₄⁻ is located. Such an alignment is not observed in complex **1** where the cavity is occupied by neutral dmcn. The encapsulation of ClO₄⁻ inside the cavity can also be inferred from the higher association constant values compared to NO₃⁻ in solution. Due to its tetrahedral topology, the ClO₄⁻ anion has greater number of interactions. Similarly, the WO₄²⁻ is located inside the hydrophobic cavity consisting of six phenyl rings of the Cu₃(dppm)₃ core. The coordination of the anion to copper centers is primarily responsible for this but weak nonbonding interactions between the oxygen atoms of WO₄²⁻ and methylene and phenyl hydrogens of dppm also play a very significant role.

Conclusion

Cu^I-dppm complexes are excellent hosts for anions. When the weakly coordinating BF₄⁻ is present, the cavity generated by the Cu₂(dppm)₂ core is occupied by a neutral guest such as dmcn. Several Cu^I-dppm complexes encapsulating oxyanions can be prepared by replacing the noncoordinating BF₄⁻. Independent synthesis of these anion-encapsulated complexes are possible starting with the corresponding Cu(II) salts. X-ray crystallographic characterization of the complexes helps in

understanding the solid-state structure of the complexes and the nature of interaction between the oxyanion and the copper-dppm core. The anchoring of the oxyanion to the core is predominantly through coordination to the metal. Noncovalent C-H...O interactions between the oxygen atoms of the oxyanion and the methylene and phenyl protons of the dppm also play a significant role. The presence of the anion is reflected in the IR spectra. The solid-state photophysical properties of these complexes are characteristic of the anion present. This property along with the lability of these complexes in solution suggest the possibility of designing an anion sensor based on Cu₂(dppm)₂ units. Addition of the oxyanion to CDCl₃ solutions of **1** results in an equilibrium reaction favoring the anion-complexed form. ¹H and ³¹P{¹H} NMR chemical shift values can be used to monitor the equilibrium.

Acknowledgment. This work was supported by a grant from CSIR (New Delhi).

Supporting Information Available: Listing of the atomic coordinates and equivalent isotropic displacement parameters, all bond lengths and angles, anisotropic displacement parameters, hydrogen coordinates and isotropic displacement parameters, intra- and intermolecular hydrogen bonding, and the emission and corresponding excitation spectra of the complexes, as well as titration curves and space-filling models of the complexes with and without the oxyanion. This material is available free of charge via the Internet at <http://pubs.acs.org>.

IC9801589